Nonaxisymmetric disturbances in compound liquid jets falling under gravity

Muhammad F. Afzaal[1] and Jamal Uddin[2,*]
[1]*Department of Chemical Engineering, Imperial College London, London SW7 2AZ, United Kingdom*
[2]*School of Mathematics, University of Birmingham, Birmingham B15 2TT, United Kingdom*
(Received 7 April 2015; revised manuscript received 28 June 2016; published 27 October 2016)

The disintegration of a compound thread of fluid can be utilized in a wide variety of applications including the production of compound droplets or capsules. In this paper we investigate the linear instability of a compound inviscid liquid jet falling under gravity in a surrounding gas with respect to nonaxisymmetric waves. We derive an analytical expression for the dispersion relation, which takes into account the non-uniform nature of the jet, and which we then solve numerically. Particular attention is paid to investigating the effects of the liquid-to-gas density ratio on the growth and development of different wave modes as well as the influence of gravity. Our results show that there exists some nonaxisymmetric long wavelength disturbances that are more unstable than their asymmetric equivalents and that the influence of gravity can alter the behavior of these modes.

DOI: 10.1103/PhysRevE.94.043114

I. INTRODUCTION

The production of capsules which encase a droplet (alternatively known as compound droplets) find a whole host of applications in modern settings. A typical example is the production of such capsules in pharmaceutics (see [1]) where the outer 'shell' may offer a mechanism for slow release of the inner core droplet material into the body or blood stream. Such compound droplets may be produced from the deformation and rupture of a compound liquid jet which has a tendency, due to surface tension forces, to breakup into spherical shaped droplets. The compound jet itself is composed of an inner thread of fluid which is completely covered by another outer immiscible liquid. This type of fluid system contain two interfaces, an inner interface separating the core and annular fluid whilst the outer interface separates the annular fluid and ambient gas regions.

Understanding the tendency of a fluid column to disintegrate into a series of periodic droplets has been a subject of interest for almost 150 years dating back to the early works of Rayleigh [2] and Savart [3]. Since then a large body of literature has accumulated investigating myriad different settings, applications, and aspects of this prototypical set-up considered by Rayleigh. A testament to the growing importance of liquid jet rupture can be gauged by the number of reviews in modern times including those of Lin [4], Eggers [5], Eggers and Villermaux [6], and Papageorgiu [7].

The presence, and consequent effects, of the surrounding gas or fluid on the rupture of a liquid jet was originally considered by Weber [8] and Tomotika [9] who investigated the instability of a liquid jet immersed in a viscous fluid. Their results identified the optimum parameter values at which the liquid jet was unstable. Later, a number of authors including Sterling and Sleicher [10], Reitz and Bracco [11], Lin and Reitz [12] investigated the influence of a surround gas on the breakup of a liquid jet identifying a number of key features including how the presence of a surrounding gas can enhance the breakup process.

Rayleigh's original analysis, which did not take into account any surrounding medium, suggested that only modes which are axisymmetric can be unstable on the surface of a liquid jet. However, in the presence of a surrounding gas (which is of particular relevance when, say, a liquid jet is assumed to be moving with high speed) experiments reveal the onset of a different type of breakup structure. In such cases nonaxisymmetric waves are found to grow with time and for sufficiently high speed jets the jet shape can become deformed. Experimental verification of this situation can be found in Hoyt and Taylor [13] where high Reynolds number jets discharging into air were observed to include nonaxisymmetric instabilities.

One-dimensional temporal instability analysis of an inviscid compound jet was considered by Sanz and Meseguer [14]. They studied the influence of surface tension ratios, density ratios, and radii ratios of inner to outer fluids and established the breakup regimes and finally compared the theoretical results with the experiment performed by Hertz and Hermanrud [15]. The capillary instability of compound jets in the presence of viscosity was presented by Radev and Tchavdarov [16]. By using two-dimensional equation of motion the influence of secondary fluid layer on the instability was investigated numerically and three types of breakup regimes were identified in this analysis.

A mathematical treatment of such nonaxisymmetric waves along a liquid jet was treated initially by Yang [17] who demonstrated that such instabilities, on a inviscid liquid jet, only occur for high Weber number values and that for sufficiently large Weber numbers nonaxisymmetric modes can be more unstable than their symmetric counterparts. Subsequently a number of authors including Ruo *et al.* [18], Avital [19], and Ibrahim [20] have considered similar situations involving the inclusion of viscosity and Chen *et al.* [21] have considered the nonaxisymmetric modes in annular jets (these authors were able to show analytically for two special cases, a very thin annular jet and an annular jet with disturbances of very small axial wavelength, that the axisymmetric instability mode has the largest growth rate). Extensions of all these works were then examined by Ruo *et al.* [22] who considered the instability of a compound liquid jet to nonaxisymmetric disturbances in the presence of a surrounding gas. A number of similar studies examining instability of compound jets can

*Corresponding author: J.Uddin@bham.ac.uk

be found in Chauhan *et al.* [23], Ramos [24], Chauhan *et al.* [25], Craster *et al.* [26], Chiu and Lin [27], and references cited therein. These authors concluded that the propagation of nonaxisymmetric waves along the compound liquid jet are similar to those of single liquid jets with the key factor influencing relative growth of nonaxisymmetric waves being the Weber number and the gas to shell density ratio.

Liquid jets which are accelerating, due to for example, rotational or gravitational forces have received less attention. Recently Amini *et al.* [28] investigated the effects of gravitational forces on a liquid jet concluding that gravitational forces can alter maximal growth rates towards shorter waves and increase cut-off frequencies. Vu *et al.* [29,30] have investigated the unsteady evolution of compound jet interfaces numerically using the front tracking and finite difference method. Their results provide good agreement with experimental results but do not take into account three dimensional effects and most notably the presence of nonaxisymmetric distortions to the jet. In this paper we examine the instability of a compound inviscid liquid jet which is falling vertically under the influence of gravity in the presence of a surrounding gas. We pay particular attention to the growth of nonaxisymmetric modes and the effects caused by the non-uniform nature of the jet.

Given the complexity of the physical set-up described above, in this paper we restrict ourselves to the simplified case of an inviscid jet and we only consider a linear temporal stability analysis. Both of these simplifications have implications on reproducing experimental results but the results presented within this paper can be used to understand the behavior of the system as a whole and in particular appreciate the influence of key parameters. The effects of viscosity in the surrounding medium are known to influence the growth rates and unstable wave numbers of disturbances (see Gordillo and Perez-Saborid [31]). However, as mentioned by those authors the neglect of viscous effects is reasonable under some conditions and provides a basis for understanding the instability of a compound jet in such cases. Additionally, viscous effects strongly influence absolute instability regions for such co-flowing systems (Herrada *et al.* [32]). Spatial stability analysis can improve upon temporal stability analysis and comparisons between theoretical results and experiments (Gonzalez and Garcia [33]). However, both temporal and spatial stability analysis are only useful if the liquid thread is in the *jetting* regime which can only be determined via a spatiotemporal analysis as conducted by Herrada *et al.* [32,34]. Global stability analysis can add yet further insight into such problems (see Theofilis [35] for a review) and has been applied to jets falling under gravity by Sauter and Buggisch [36] and Rubio-Rubio *et al.* [37] although de Luca *et al.* [38] suggest that jet breakup could be linked to the amplification of the so-called pseudo-modal disturbances rather than exponentially growing modal disturbances. In such cases the comparisons between linear theory and experiments can prove limited especially when the jets become very thin as discussed by Javadi *et al.* [39].

II. PROBLEM FORMULATION

We begin by considering an inviscid compound jet which emerges from a concentric tube with exit velocity U and moves in a surrounding gas (which is initially stationary). The initial outer radius of the compound jet is a with the inner jet having a smaller initial radius χa, where $0 < \chi < 1$. It is assumed that the compound jet, after emerging from a circular orifice, falls in a vertical direction under the influence of gravity. It is also assumed that all the fluids are incompressible and immiscible. The geometry of the compound jet is described in a cylindrical coordinate system (r,θ,x), where r is the radial component, θ is the azimuthal component and x represents the axial direction of the jet (see Fig. 1). The velocity vector describing the flow can be written as $\mathbf{u^{[z]}} = (\mathbf{w^{[z]}},\mathbf{v^{[z]}},\mathbf{u^{[z]}})$, where the subscript $z = I$ is for the inner fluid, $z = O$ is for the outer fluid and $z = A$ is for the surrounding gas. Here we denote $r = R(x,t)$ as the interface of inner fluid with the outer one, $r = S(x,t)$ as the interface of outer fluid with the surrounding gas, $\sigma^{[I]}$ is the surface tension at the interface $r = R(x,t)$, and $\sigma^{[O]}$ is the surface tension at the interface $r = S(x,t)$. The density of the fluids is denoted by $\rho^{[z]}$, and the pressure and the time are denoted as $p^{[z]}$ and t, respectively. The gravity is taken as $\mathbf{g} = (0,0,g)$. In addition, the surface tensions $\sigma^{[I]}$ and $\sigma^{[O]}$ are assumed to be constant at the inner and the outer interface, respectively.

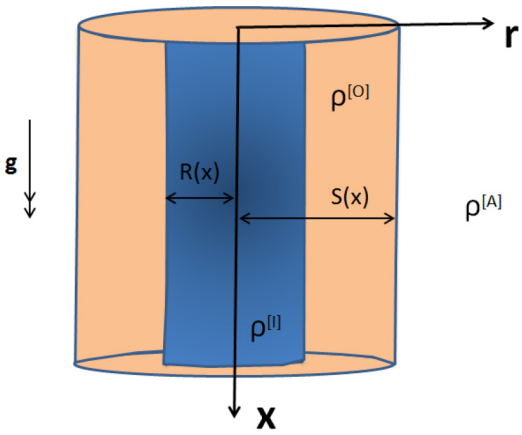

FIG. 1. A schematic of the compound jet depicting the inner and outer jets with some of the parameter values.

The continuity equation and the Euler equation, which describe the resulting dynamics of the compound jet, are given by

$$\frac{\partial u^{[z]}}{\partial x} + \frac{\partial w^{[z]}}{\partial r} + \frac{w^{[z]}}{r} + \frac{1}{r}\frac{\partial v^{[z]}}{\partial \theta} = 0, \tag{1}$$

$$\frac{\partial u^{[z]}}{\partial t} + u^{[z]}\frac{\partial u^{[z]}}{\partial x} + w^{[z]}\frac{\partial u^{[z]}}{\partial r} + \frac{v^{[z]}}{r}\frac{\partial u^{[z]}}{\partial \theta} = -\frac{1}{\rho^{[z]}}\frac{\partial p^{[z]}}{\partial x} + (\delta_{\mathbf{Iz}} + \delta_{\mathbf{Oz}})g, \tag{2}$$

$$\frac{\partial v^{[z]}}{\partial t} + u^{[z]}\frac{\partial v^{[z]}}{\partial x} + w^{[z]}\frac{\partial v^{[z]}}{\partial r} + \frac{v^{[z]}}{r}\frac{\partial v^{[z]}}{\partial \theta} + \frac{v^{[z]}w^{[z]}}{r} = -\frac{1}{\rho^{[z]}}\frac{1}{r}\frac{\partial p^{[z]}}{\partial \theta}, \tag{3}$$

and

$$\frac{\partial w^{[z]}}{\partial t}+u^{[z]}\frac{\partial w^{[z]}}{\partial x}+w^{[z]}\frac{\partial w^{[z]}}{\partial r}+\frac{v^{[z]}}{r}\frac{\partial w^{[z]}}{\partial \theta}-\frac{(v^{[z]})^2}{r} =-\frac{1}{\rho^{[z]}}\frac{\partial p^{[z]}}{\partial r}, \tag{4}$$

where $\delta_{\mathbf{Iz}}$ and $\delta_{\mathbf{Oz}}$ are the Kronecker δ symbols with free index z. These equations are supplemented by the kinematic conditions and the normal stress conditions. The kinematic conditions, at the interface $r=R(x,t)$, are given by

$$w^{[z]}=\frac{\partial R}{\partial t}+u^{[z]}\frac{\partial R}{\partial x}+\frac{v^{[z]}}{r}\frac{\partial R}{\partial \theta}, \tag{5}$$

where $z=I,O$. Similarly, the kinematic conditions, at the interface $r=S(x,t)$, are given by

$$w^{[z]}=\frac{\partial S}{\partial t}+u^{[z]}\frac{\partial S}{\partial x}+\frac{v^{[z]}}{r}\frac{\partial S}{\partial \theta}, \tag{6}$$

where $z=O,A$. For inviscid fluids, we have the classical free surface condition of constant pressure and hence zero tangential stress condition. The normal stress conditions, at the interfaces $r=R(x,t)$ and $r=S(x,t)$, are

$$p^{[I]}-p^{[O]}=\sigma^{[I]}\kappa^{[I]} \tag{7}$$

and

$$p^{[O]}-p^{[A]}=\sigma^{[O]}\kappa^{[O]}, \tag{8}$$

respectively, where $\kappa^{[I]}$ is the curvature of the inner free surface and $\kappa^{[O]}$ is the curvature of the outer free surface, which are given by

$$\kappa^{[I]}=\frac{\partial}{\partial x}\left(-\frac{1}{E^{[I]}}\frac{\partial R}{\partial x}\right)+\frac{\partial}{\partial r}\left(\frac{r}{E^{[I]}}\right)+\frac{\partial}{\partial \theta}\left(-\frac{1}{rE^{[I]}}\frac{\partial R}{\partial \theta}\right), \tag{9}$$

$$\kappa^{[O]}=\frac{\partial}{\partial x}\left(-\frac{1}{E^{[O]}}\frac{\partial S}{\partial x}\right)+\frac{\partial}{\partial r}\left(\frac{r}{E^{[O]}}\right)+\frac{\partial}{\partial \theta}\left(-\frac{1}{rE^{[O]}}\frac{\partial S}{\partial \theta}\right), \tag{10}$$

where

$$E^{[I]}=\left(1+\left(\frac{\partial R}{\partial x}\right)^2+\frac{1}{r^2}\left(\frac{\partial R}{\partial \theta}\right)^2\right)^{\frac{1}{2}}, \tag{11}$$

$$E^{[O]}=\left(1+\left(\frac{\partial S}{\partial x}\right)^2+\frac{1}{r^2}\left(\frac{\partial S}{\partial \theta}\right)^2\right)^{\frac{1}{2}}. \tag{12}$$

We can non-dimensionalize the velocity components with the initial jet velocity U at the tube exit, so we have $\bar{w}^{[z]}=w^{[z]}/U$, $\bar{v}^{[z]}=v^{[z]}/U$, and $\bar{u}^{[z]}=u^{[z]}/U$, radial lengths with the outer jet radius a so that $\bar{r}=r/a$, the azimuthal component $\bar{\theta}=\theta$ and the axial length with a characteristic wavelength L (typically much greater than a) in the axial direction as $\bar{x}=x/L$. The time and the pressure are scaled by $\bar{t}=tU/L$ and $\bar{p}^{[z]}=p^{[z]}/\rho^{[O]}U^2$, respectively. By assuming the jet is slender, we define a small parameter ϵ as $\epsilon=a/L\ll 1$. The dimensionless forms of the inner and the outer radii of the jet at the nozzle are $R(0,t)=\chi$ and $S(0,t)=1$, respectively.

After dropping the overbars, the resulting dimensionless continuity and Euler equations can be written as

$$\frac{\partial u^{[z]}}{\partial x}+\frac{1}{\epsilon}\frac{\partial w^{[z]}}{\partial r}+\frac{1}{\epsilon}\frac{w^{[z]}}{r}+\frac{1}{\epsilon r}\frac{\partial v^{[z]}}{\partial \theta}=0, \tag{13}$$

$$\frac{\partial u^{[z]}}{\partial t}+u^{[z]}\frac{\partial u^{[z]}}{\partial x}+\frac{w^{[z]}}{\epsilon}\frac{\partial u^{[z]}}{\partial r}+\frac{v^{[z]}}{\epsilon r}\frac{\partial u^{[z]}}{\partial \theta} =-((\delta_{\mathbf{Iz}})\rho+(\delta_{\mathbf{Az}})\rho^G)\frac{\partial p^{[z]}}{\partial x}+(\delta_{\mathbf{Iz}}+\delta_{\mathbf{Oz}})\frac{1}{F^2}, \tag{14}$$

$$\frac{\partial v^{[z]}}{\partial t}+u^{[z]}\frac{\partial v^{[z]}}{\partial x}+\frac{w^{[z]}}{\epsilon}\frac{\partial v^{[z]}}{\partial r}+\frac{v^{[z]}}{\epsilon r}\frac{\partial v^{[z]}}{\partial \theta}+\frac{v^{[z]}w^{[z]}}{\epsilon r} =-((\delta_{\mathbf{Iz}})\rho+(\delta_{\mathbf{Az}})\rho^G)\frac{1}{\epsilon r}\frac{\partial p^{[z]}}{\partial \theta}, \tag{15}$$

and

$$\frac{\partial w^{[z]}}{\partial t}+u^{[z]}\frac{\partial w^{[z]}}{\partial x}+\frac{w^{[z]}}{\epsilon}\frac{\partial w^{[z]}}{\partial r}+\frac{v^{[z]}}{\epsilon r}\frac{\partial w^{[z]}}{\partial \theta}-\frac{(v^{[z]})^2}{\epsilon r} =-((\delta_{\mathbf{Iz}})\rho+(\delta_{\mathbf{Az}})\rho^G)\frac{1}{\epsilon}\frac{\partial p^{[z]}}{\partial r}, \tag{16}$$

where $\rho^G=\rho^{[A]}/\rho^{[O]}$ is the density ratio of the surrounding gas to the outer fluid, $\delta_{\mathbf{Iz}},\delta_{\mathbf{Oz}}$, and $\delta_{\mathbf{Az}}$ are the Kronecker δ symbols with free index z. The dimensionless kinematic conditions, at the interface $r=R(x,t)$ and $r=S(x,t)$, are given by

$$w^{[z]}=\frac{\partial R}{\partial t}+u^{[z]}\frac{\partial R}{\partial x}+\frac{v^{[z]}}{\epsilon r}\frac{\partial R}{\partial \theta}, \tag{17}$$

where $z=I,O$ and

$$w^{[z]}=\frac{\partial S}{\partial t}+u^{[z]}\frac{\partial S}{\partial x}+\frac{v^{[z]}}{\epsilon r}\frac{\partial S}{\partial \theta}, \tag{18}$$

where $z=O,A$, respectively. The dimensionless normal stress conditions, at the interfaces $r=S(x,t)$ and $r=R(x,t)$, are

$$p^{[O]}-p^{[A]}=\frac{1}{\mathrm{We}}\frac{\partial}{\partial x}\left(-\frac{\epsilon^2}{E^{[O]}}\frac{\partial S}{\partial x}\right)+\frac{\partial}{\partial r}\left(\frac{r}{E^{[O]}}\right)+\frac{\partial}{\partial \theta}\left(-\frac{1}{rE^{[O]}}\frac{\partial S}{\partial \theta}\right) \tag{19}$$

and

$$p^{[I]}-p^{[O]}=\frac{\sigma}{We}\frac{\partial}{\partial x}\left(-\frac{\epsilon^2}{E^{[I]}}\frac{\partial R}{\partial x}\right)+\frac{\partial}{\partial r}\left(\frac{r}{E^{[I]}}\right)+\frac{\partial}{\partial \theta}\left(-\frac{1}{rE^{[I]}}\frac{\partial R}{\partial \theta}\right), \tag{20}$$

respectively, where

$$E^{[I]}=\left(1+\epsilon^2\left(\frac{\partial R}{\partial x}\right)^2+\frac{1}{r^2}\left(\frac{\partial R}{\partial \theta}\right)^2\right)^{\frac{1}{2}}, \tag{21}$$

$$E^{[O]}=\left(1+\epsilon^2\left(\frac{\partial S}{\partial x}\right)^2+\frac{1}{r^2}\left(\frac{\partial S}{\partial \theta}\right)^2\right)^{\frac{1}{2}}, \tag{22}$$

and $\sigma=\sigma^{[I]}/\sigma^{[O]}$ is the ratio of surface tension between inner and outer fluid interfaces. There are two key nondimensional numbers; namely the Weber number $We=\rho^{[O]}U^2a/\sigma^{[I]}$ which measures the ratio of surface tension forces to inertia and

the Froude number $F = gL/U^2$ which measures the relative importance of gravity forces over inertia.

III. ASYMPTOTIC FORM OF THE STEADY STATE SOLUTIONS

In order to find the steady state solutions, we consider motionless gas [22], that is $\mathbf{u}^{[\mathbf{A}]} = (0,0,0)$, and expand our variables using an asymptotic slender jet steady expansion of the form

$$\{w^{[z]},v^{[z]},u^{[z]},p^{[z]}\} = \{0,0,(\delta_{Iz}+\delta_{Oz})u_0^{[z]}(x), \times p_0^{[z]}(r,\theta,x)\} + (\epsilon r)\{(\delta_{Iz}+\delta_{Oz})[w_1^{[z]}(\theta,x), \times v_1^{[z]}(\theta,x),u_1^{[z]}(\theta,x)],p_1^{[z]}(\theta,x)\} + O(\epsilon^2 r^2), \quad (23)$$

$$\{R,S\} = \{R_0(x),S_0(x)\} + \epsilon\{R_1(\theta,x),S_1(\theta,x)\} + O(\epsilon^2). \quad (24)$$

Substituting the above asymptotic expansions in Eqs. (13)–(22), consequently, the leading order continuity equation for the inner and outer fluids is

$$w_1^{[z]} = -\frac{1}{2}\frac{\partial u_0^{[z]}}{\partial x}, \quad (25)$$

where $z = I,O$. The leading order kinematic conditions (17) and (18), at $r = R(x)$ and $r = S(x)$, give

$$\frac{\partial}{\partial x}\left(R_0^2 u_0^{[I]}\right) = 0 \quad (26)$$

and

$$\frac{\partial}{\partial x}\left((S_0^2 - R_0^2)u_0^{[O]}\right) = 0, \quad (27)$$

respectively. The leading order normal stress conditions (19) and (20), at $r = S(x,t)$ and $r = R(x,t)$, yield

$$p_0^{[O]} = \frac{1}{S_0\mathrm{We}} + p_0^{[A]}, \quad \text{and} \quad p_0^{[I]} = \frac{1}{\mathrm{We}}\left(\frac{\sigma}{R_0} + \frac{1}{S_0}\right) + p_0^{[A]}, \quad (28)$$

respectively. The leading order azimuthal and radial momentum equations (15) and (16) give $\partial p_0^{[z]}/\partial\theta = 0$ and $\partial p_0^{[z]}/\partial r = 0$, respectively. We now substitute Eq. (28) in the axial momentum equation (14) for the inner and the outer fluids, which after using the boundary conditions at the nozzle, which are $u_0^{[I]} = u_0^{[O]} = S_0 = 1$ and $R_0 = \chi$, yields

$$u_0^{[I]} = \sqrt{1 + \frac{2x}{F^2} + \frac{1}{\rho\mathrm{We}}\left(1 + \frac{\sigma}{\chi} - \frac{\sigma}{R_0} - \frac{1}{S_0}\right)} \quad (29)$$

and

$$u_0^{[O]} = \sqrt{1 + \frac{2x}{F^2} + \frac{1}{\rho\mathrm{We}}\left(1 - \frac{1}{S_0}\right)}. \quad (30)$$

Similarly one may integrate Eqs. (26) and (27) and then use the boundary conditions at the nozzle to derive expressions for R_0 and S_0 and then consequently use Eq. (28) to arrive at expressions for $p_0^{[O]}$ and $p_0^{[I]}$ [40–42].

IV. LINEAR ANALYSIS

We now consider a linear temporal instability analysis of a nonaxisymmetric compound liquid jet moving in a surrounding gas. We consider small perturbations to the steady state solutions found in the previous section. We now note that the evolution of the jet depends on a length scale $x = O(1)$, but

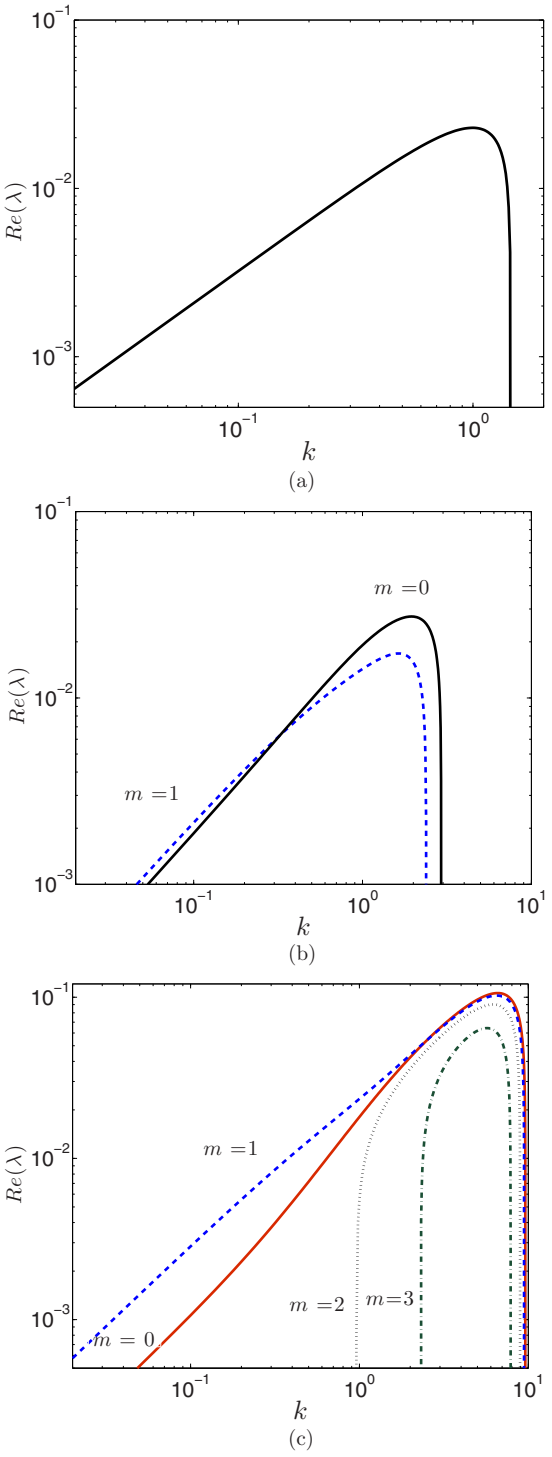

FIG. 2. Growth rate of the disturbances versus wave number at $x = 0$. Other parameters are $\rho = 1, \rho^G = 0.001, \sigma = 1, F = 1$, and $\chi = 0.4$: (a) We = 1000, (b) We = 3000, (c) We = 10 000.

unstable disturbances along the jet typically have wavelengths which are much smaller (see [2]) and are comparable to ϵ when $x = O(1)$. We therefore consider traveling short waves of the form $e^{\lambda\hat{t}+i(k\hat{x}+m\theta)}$, where $k = k(x) = O(1)$ and $\lambda = \lambda(x) = O(1)$ are the frequency and wave number of disturbances. Additionally, $\hat{x} = x/\epsilon$ and $\hat{t} = t/\epsilon$ are small length and time scales. Thus, we have a multiple scale formulation as the perturbations grow along the jet having wavelength of $O(\epsilon)$. Now we introduce small time dependent perturbations to the steady state solutions which take the form

$$(w^{[z]},v^{[z]},u^{[z]},p^{[z]}) = \left(0,0,(\delta_{Iz}+\delta_{Oz})u_0^{[z]},p_0^{[z]}\right) + \Lambda(\tilde{w}(r)^{[z]},\tilde{v}(r)^{[z]},\tilde{u}(r)^{[z]},\tilde{p}(r)^{[z]})\Omega, \tag{31}$$

$$(R,S) = (R_0,S_0) + \Lambda(\tilde{R},\tilde{S})\Omega, \tag{32}$$

where $\Omega = \exp(\lambda\hat{t} + i(k\hat{x} + m\theta))$ and $0 < \Lambda \ll \epsilon$. Substituting the expansions (31) and (32) into Eqs. (13)–(22) yields a set of equations which are given in the Appendix. Nontrivial solutions to this set of equations are given by the dispersion relation

$$D(k,\lambda;We,m,\sigma,\rho,\rho^G,\chi,x) = 0. \tag{33}$$

We note that the above dispersion relation does not explicitly depend on the Froude number F and instead this dependency only enters via the steady state solutions $u_0^{[O]},u_0^{[I]},R_0$, and S_0 from the previous section. In general these will vary along x and will be different for different values of F.

V. RESULTS AND DISCUSSION

The dispersion relation we obtain above is a quartic in λ and reduces to the one obtained by Yang [17] when we set $\sigma = 0, S_0 = R_0 = 1$, and $\rho = 1$. For arbitrary values of the parameters we solve this equation using Ferrari's method [43] to obtain the most unstable modes. We are interested in investigating parameter regimes which resemble those used in the experiments of Hertz and Hermanrud [15] (which is the most comprehensive experimental compound jet paper to date) and for this purpose we consider jets with typical radii $R \sim 10^{-3}$–10^{-5} m, typical velocities $U \sim 10$ m/s, and typical dynamic viscosities 1–10 cP. This leads to an effective Reynolds number Re $\sim O(10^3)$ which allows us to neglect viscous effects. Moreover, typical surface tension values used were in the range $\sigma_0 \sim 20$–72 dyn/cm which leads to values for the Weber number as We $\sim O(10^3)$. As we increase the Weber number we see the sinuous mode $m = 1$ first becomes unstable (and indeed is more unstable than the symmetric mode) for long wavelength disturbances. As the Weber number is further increased we notice the appearance of higher order unstable modes while the wave number range of instability also increases. We demonstrate these trends in Fig. 2. Figure 3 presents the growth rate of disturbances for various Froude numbers at a certain distance along the jet at $x = 1$ for the sinuous mode $m = 1$, where we can see that the growth rate of disturbances decreases with a decrease in Froude number.

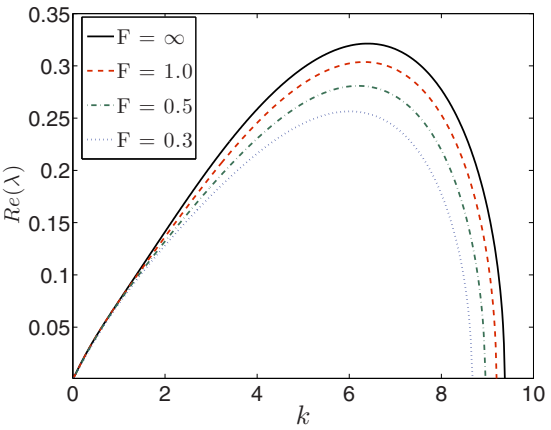

FIG. 3. Growth rate of the disturbances versus wave number for various values of Froude number. Other parameters are $\rho = 1$, $\rho^G = 0.01, \sigma = 1, x = 1, \chi = 0.5, m = 1$, and We $= 1000$.

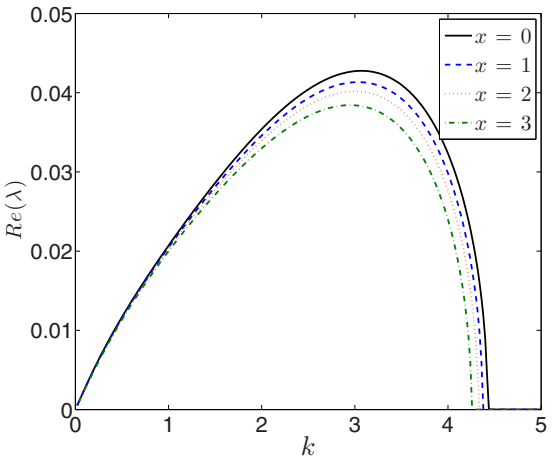

FIG. 4. Growth rate of the disturbances versus wave number at various locations of the jet. Other parameters are $\rho = 1, \rho^G = 0.001$, $\sigma = 1, F = 1, \chi = 0.4, m = 1$, and We $= 3000$.

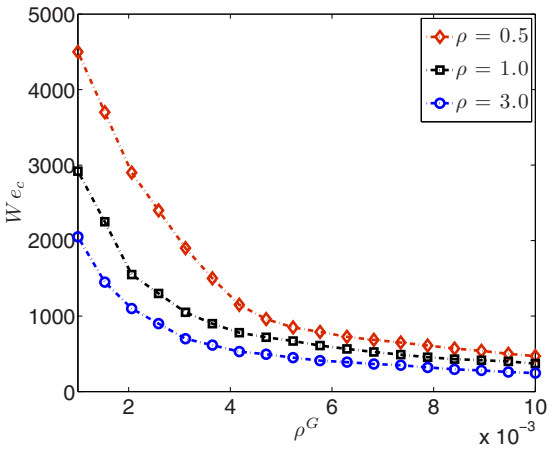

FIG. 5. Critical values of the Weber number for the growing nonaxisymmetric mode versus the gas to shell liquid density ratios for various values of liquid-liquid density ratios at $x = 0$. Other parameters are $m = 1, \sigma = 1, F = 1$, and $\chi = 0.5$.

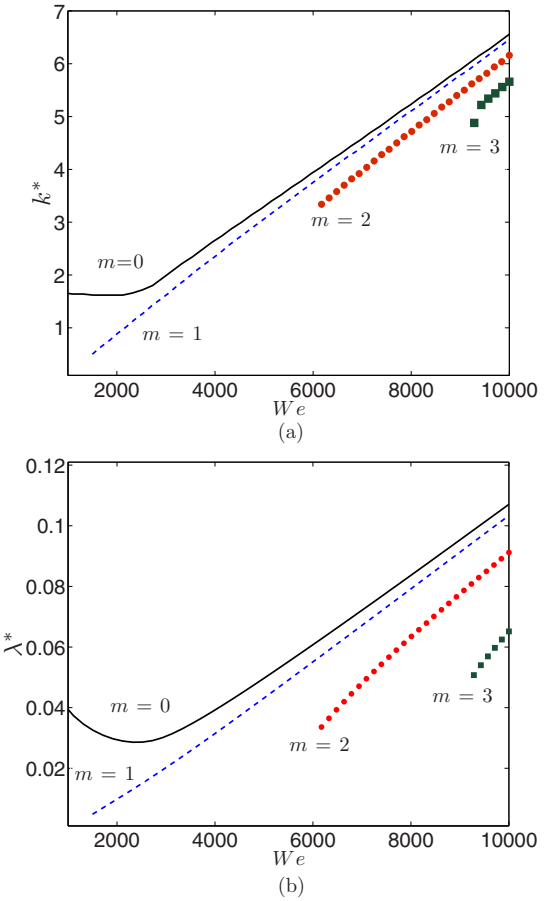

FIG. 6. (a) Maximum wave number k^* versus the Weber number for various values of m. (b) Maximum growth rate of disturbances λ^* versus the Weber number for various values of m. Other parameters are $\rho = 1, \sigma = 1, \rho^G = 0.001, F = 1$, and $\chi = 0.4$.

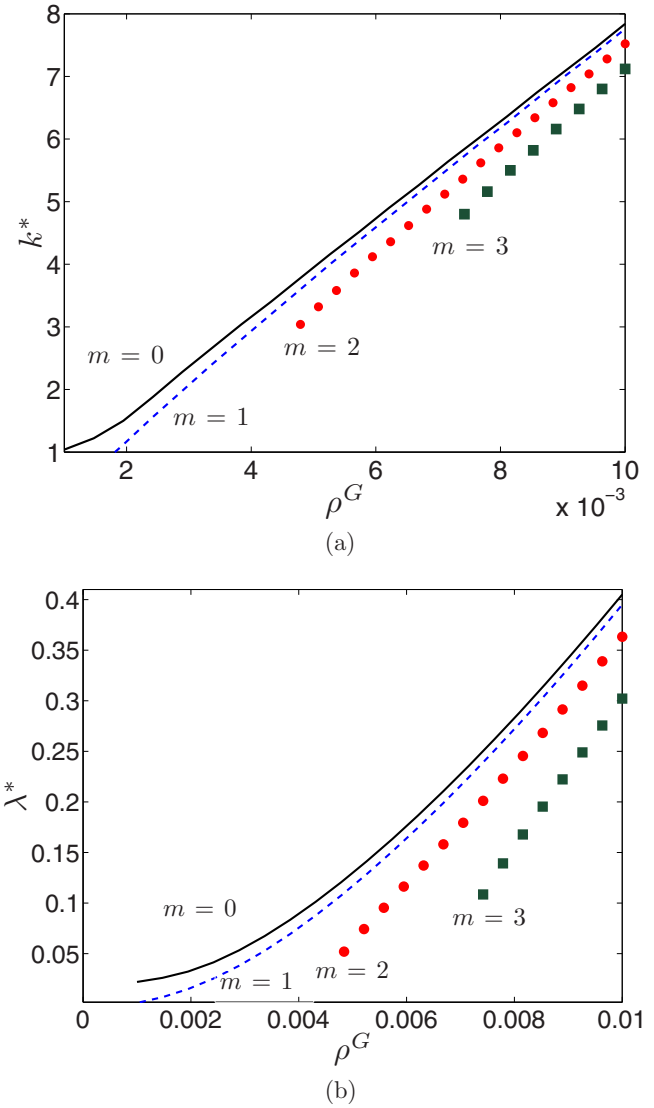

FIG. 7. (a) Maximum wave number k^* versus the gas to shell liquid density ratios for various values of m. (b) Maximum growth rate of disturbance λ^* versus the gas to shell liquid density ratios for various values of m. Other parameters are $\rho = 1, \sigma = 1$, $\mathrm{We} = 10\,000, F = 1$, and $\chi = 0.4$.

Conversely, the growth rate increases for the smaller values of Weber number at $m = 0$ as the sinus mode does not grow for the smaller values of Weber number. We can see how the growth rate of disturbances are affected as we move down the jet in Fig. 4 where we plot the growth rate of the sinuous mode for a range of locations along the jet. The range of unstable wave numebrs for the sinuous mode decreases with distance along the jet as does the growth rate of disturbances. In Fig. 5 we plot how changing the density ratio between the surrounding gas and the outer fluid affects the critical Weber number for various liquid-liquid density ratios (between the inner and the outer jet). From this figure we see that as we increases the liquid-liquid density ratios ρ we see a reduction in the critical Weber number for all shell to gas density ratios (the density ratio between the surrounding gas and the outer fluid) ρ^G with the largest differences occurring when the shell to gas density ratio is smallest. In Fig. 6 we plot both the most unstable wave number (that is the wave number $k = k^*$ at which the growth rate is maximal) as well as the growth rate itself versus Weber numbers for various values of m. The appearance of higher modes can be seen as the Weber number increases and only for the highest Weber numbers presented $\sim 10^4$ do modes $m = 3$ appear. Since only the *most* unstable wave mode and its associated growth rate are plotted in this figure we do not observe the fact that there are wave modes where the sinuous mode $m = 1$ is in fact more unstable than the symmetric mode which is more clearly seen in Fig. 2. We do a similar analysis in Fig. 7 where we plot the growth rate and the most unstable wave number versus gas to shell density ratios. We observe a similar trend in this case for increasing values of ρ^G.

VI. CONCLUSION

We have formulated the governing equations for an inviscid compound liquid jet which is falling under gravity in the presence of a surrounding gas. The model equations are then utilised to find a steady state solution which is dependent on axial location. Small linear nonaxisymmetric disturbances about this steady state are then considered to yield a dispersion relation relating the growth of disturbances to the associated

wave number for different nonaxisymmetric modes m. We have shown that higher modes are present when the Weber number is sufficiently high and that for certain ranges of the wave number the sinuous mode can be greater then the symmetric mode.

APPENDIX

The Appendix details the dispersion relation (33). We substitute the expansions (31) and (32) into the non-dimensionalized form of Eqs. (13)–(22), which yields at $O(\Lambda/\epsilon)$:

$$ik\tilde{u}^{[z]} + \frac{\partial \tilde{w}^{[z]}}{\partial r} + \frac{\tilde{w}^{[z]}}{r} = 0, \tag{A1}$$

$$\left(\lambda + ik(\delta_{\mathbf{Iz}} + \delta_{\mathbf{Oz}})u_0^{[z]}\right)\tilde{u}^{[z]} = -((\delta_{\mathbf{Iz}})\rho + (\delta_{\mathbf{Az}})\rho^G)\tilde{p}^{[z]}ik, \tag{A2}$$

$$\left(\lambda + ik(\delta_{\mathbf{Iz}} + \delta_{\mathbf{Oz}})u_0^{[z]}\right)\tilde{v}^{[z]} = -((\delta_{\mathbf{Iz}})\rho + (\delta_{\mathbf{Az}})\rho^G)\tilde{p}^{[z]}ik, \tag{A3}$$

$$\left(\lambda + ik(\delta_{\mathbf{Iz}} + \delta_{\mathbf{Oz}})u_0^{[z]}\right)\tilde{w}^{[z]} = -(\delta_{\mathbf{Iz}}\rho + \delta_{\mathbf{Az}}\rho^G)\frac{\partial \tilde{p}^{[z]}}{\partial r}, \tag{A4}$$

$$\tilde{w}^{[z]} = \left(\lambda + iku_0^{[z]}\right)\tilde{R} \quad \text{for} \quad z = I, O, \tag{A5}$$

$$\tilde{w}^{[z]} = \left(\lambda + ik(\delta_{\mathbf{Oz}})u_0^{[z]}\right)\tilde{S} \quad \text{for} \quad z = O, A, \tag{A6}$$

$$\tilde{p}^{[I]} - \tilde{p}^{[O]} = \frac{\sigma}{\mathrm{We}}\left(k^2 - \frac{1}{R_0^2}\right)\tilde{R}, \tag{A7}$$

$$\tilde{p}^{[O]} - \tilde{p}^{[A]} = \frac{1}{\mathrm{We}}\left(k^2 - \frac{1}{S_0^2}\right)\tilde{S}. \tag{A8}$$

Using Eqs. (A2) and (A4) to eliminate $\tilde{p}^{[z]}$ we get $\tilde{w}^{[z]} = \frac{1}{ik}\frac{\partial \tilde{u}^{[z]}}{\partial r}$ and similarly Eqs. (A2) and (A3) gives $\tilde{v}^{[z]} = \frac{\tilde{u}^{[z]}}{rk}$. By substituting these result in Eq. (A1), we have

$$\frac{\partial^2 \tilde{u}^{[z]}}{\partial r^2} + \frac{1}{r}\frac{\partial \tilde{u}^{[z]}}{\partial r} - (m^2 + k^2)\tilde{u}^{[z]} = 0, \tag{A9}$$

which has solution

$$\tilde{u}^{[z]} = C^{[z]}I_m(kr) + D^{[z]}K_m(kr). \tag{A10}$$

By using the value of $\tilde{u}^{[z]}$, we are able to get

$$\tilde{w}^{[z]} = \frac{1}{ik}(C^{[z]}I'_m(kr) - D^{[z]}K'_m(kr)). \tag{A11}$$

By using Eq. (A2) in Eq. (A10), yields

$$\tilde{p}^{[z]} = \frac{-\left(\lambda + ik(\delta_{\mathbf{Iz}} + \delta_{\mathbf{Oz}})u_0^{[z]}\right)}{ik(\delta_{Iz}\rho + \delta_{\mathbf{Az}}\rho^G)}(C^{[z]}I_m(kr) + D^{[z]}K_m(kr)), \tag{A12}$$

where $I_m(kr)$ and $K_m(kr)$ are the modified Bessel functions of first and second kind, respectively. To avoid the singularities, and to ensure finite values at $r = 0$, we require that $D^{[I]}$ and $C^{[A]}$ will be equal to zero.

Substituting the values of $\tilde{w}^{[z]}$ in Eqs. (A5) and (A6), yields

$$\frac{1}{ik}(C^{[I]}I'_m(kR_0)) = \left(\lambda + iku_0^{[I]}\right)\tilde{R}, \tag{A13}$$

$$\frac{1}{ik}(C^{[O]}I'_m(kR_0) - D^{[O]}K'_m(kR_0)) = \left(\lambda + iku_0^{[O]}\right)\tilde{R}, \tag{A14}$$

$$\frac{1}{ik}(C^{[O]}I'_m(kS_0) - D^{[O]}K'_m(kS_0)) = \left(\lambda + iku_0^{[O]}\right)\tilde{S}, \tag{A15}$$

$$\frac{1}{ik}(-D^{[A]}K'_m(kS_0)) = (\lambda)\tilde{S}. \tag{A16}$$

Similarly, using the values of $\tilde{p}^{[z]}$ from Eq. (A12) in Eqs. (A7) and (A8), we get

$$\frac{-\left(\lambda + iku_0^{[I]}\right)}{ik\rho}(C^{[I]}I_m(kR_0)) + \frac{\left(\lambda + iku_0^{[O]}\right)}{ik}(C^{[O]}I_m(kR_0) + D^{[O]}K_m(kR_0)) = \frac{\sigma}{\mathrm{We}}\left(k^2 - \frac{1}{R_0^2}\right)\tilde{R}, \tag{A17}$$

$$\frac{-\left(\lambda + iku_0^{[O]}\right)}{ik}(C^{[O]}I_m(kR_0) + D^{[O]}K_m(kR_0)) + \frac{\lambda}{ik\rho^G}(D^{[A]}K_m(kR_0)) = \frac{1}{\mathrm{We}}\left(k^2 - \frac{1}{S_0^2}\right)\tilde{S}. \tag{A18}$$

We can write Eqs. (A13)–(A18) as

$$\mathbf{By} = \mathbf{0}, \tag{A19}$$

where

$$\mathbf{B} = \begin{bmatrix} \frac{1}{ik}(I'_m(kR_0)) & 0 & 0 & 0 & -\lambda + iku_0^{[I]} & 0 \\ 0 & \frac{1}{ik}(I'_m(kR_0)) & -\frac{1}{ik}(K'_m(kR_0)) & 0 & -\lambda + iku_0^{[O]} & 0 \\ 0 & \frac{1}{ik}(I'_m(kR_0)) & -\frac{1}{ik}(K'_m(kR_0)) & 0 & 0 & -\lambda + iku_0^{[O]} \\ 0 & 0 & 0 & \frac{1}{ik}(I'_m(kR_0)) & 0 & -\lambda \\ \frac{-\left(\lambda + iku_0^{[I]}\right)}{ik\rho}I_m(kR_0) & \frac{\left(\lambda + iku_0^{[O]}\right)}{ik}I_m(kR_0) & \frac{\left(\lambda + iku_0^{[O]}\right)}{ik}K_m(kR_0) & 0 & -\frac{\sigma}{\mathrm{We}}\left(k^2 - \frac{1}{R_0^2}\right) & 0 \\ 0 & \frac{-\left(\lambda + iku_0^{[O]}\right)}{ik}I_m(kR_0) & \frac{-\left(\lambda + iku_0^{[O]}\right)}{ik}K_m(kR_0) & \frac{\lambda}{ik\rho^G}K_m(kR_0) & 0 & -\frac{1}{\mathrm{We}}\left(k^2 - \frac{1}{S_0^2}\right) \end{bmatrix}$$

and

$$\mathbf{y}^\top = [C^{[O]}C^{[I]}D^{[O]}D^{[A]}\tilde{R}\tilde{S}].$$

The determinant of the matrix then gives the expression in Eq. (33).

[1] A. M. Ganan-Calvo, J. M. Montanero, L. Martin-Banderas, and M. Flores-Mosquera, Building functional materials for healthcare and pharmacy from microfluidic principles and flow focusing, Adv. Dru. Del. Rev. **65**, 1447 (2013).

[2] W. S. Rayleigh, On the instability of jets, Proc. Lond. Math. Soc. **10**, 4 (1878).

[3] F. Savart, Memoire sur la constitution des veines liquides lancees par des orices circulaires en mince paroi, Ann. Chim. **53**, 337 (1833).

[4] S. P. Lin, *Breakup of Liquid Sheets and Jets* (Cambridge University Press, Cambridge, 2003).

[5] J. Eggers, Nonlinear dynamics and breakup of free surface flows, Rev. Mod. Phys. **69**, 865 (1997).

[6] J. Eggers and E. Villermaux, Physics of liquid jets, Rep. Prog. Phys. **71**, 036601 (2008).

[7] D. T. Papageorgiu, Interfacial phenomena and the Marangoni effect, in *Hydrodynamics of Surface Tension Dominated Flows*, edited by M. Velarde *et al.* (Springer-Verlag, Wien, 2002), pp. 41–88.

[8] C. Weber, Zum zerfall eines Flussigkeitsstrahles, Z. Angew. Math. Mech. **11**, 136 (1931).

[9] S. Tomotika, On the stability of a cylindrical thread of a viscous liquid surrounded by another viscous liquid, Proc. R. Soc. London A **150**, 322 (1936).

[10] A. M. Sterling and C. A. Sleicher, The instability of capillary jets, J. Fluid Mech. **68**, 477 (1975).

[11] R. D. Reitz and F. V. Bracco, Mechanism of atomization of a liquid jet, Phys. Fluids **25**, 1730 (1982).

[12] S. P. Lin and R. D. Reitz, Drop and spray formation from a liquid jet, Annu. Rev. Fluid Mech. **30**, 85 (1998).

[13] J. W. Hoyt and J. J. Taylor, Waves on water jets, J. Fluid Mech. **83**, 119 (1977).

[14] A. Sanz and J. Meseguer, One-dimensional analysis of the compound jet, J. Fluid Mech. **159**, 55 (1985).

[15] C. H. Hertz and B. Hermanrud, A liquid compound jet, J. Fluid Mech. **131**, 271 (1983).

[16] S. Radev and B. Tchavdarov, Linear capillary instability of compound jets, Int. J. Multiphase Flow **14**, 67 (1988).

[17] H. Q. Yang, Asymmetric instability of a liquid jet, Phys. Fluids **4**, 681 (1992).

[18] A. C. Ruo, M. H. Chang, and F. Chen, On the nonaxisymmetric instability of round liquid jets, Phys. Fluids **20**, 062105 (2008).

[19] E. Avital, Asymmetric instability of a viscid capillary jet in an inviscid media, Phys. Fluids **7**, 1162 (1995).

[20] E. A. Ibrahim, Asymmetric instability of a viscous liquid jet, J. Colloid Interface Sci. **189**, 181 (1997).

[21] F. Chen, J.-Y. Tsaur, F. Durst, and S. K. Das, On the axisymmetry of annular jet instabilities, J. Fluid Mech. **488**, 355 (2003).

[22] A. C. Ruo, F. Chen, and M. H. Chang, Linear instability of compound jets with nonaxisymmetric disturbances, Phys. Fluids **21**, 012101 (2009).

[23] A. Chauhan, C. Maldarelli, D. S. Rumschitzki, and D. T. Papageorgiou, Temporal and spatial instability of an inviscid compound jet, Rhelog. Acta **35**, 567 (1996).

[24] J. I. Ramos, Asymptotic analysis of compound liquid jets at low Reynolds numbers, Appl. Math. Comput. **100**, 223040 (1999).

[25] A. Chauhan, C. Maldarelli, D. T. Papageorgiou, and D. S. Rumschitzki, Temporal instability of compound threads and jets, J. Fluid Mech. **420**, 1 (2000).

[26] R. V. Craster, O. V. Matar, and D. T. Papageorgiou, Pinchoff and satellite formation in compound viscous threads, J. Fluid Mech. **533**, 95124 (2005).

[27] S. Chiu and T. Lin, Breakup of compound liquid jets under periodic excitation at small core-to-shell mass ratio, J. Chin. Inst. Eng. **31**, 1 (2008).

[28] G. Amini, M. Ihme, and A. Dolatabadi, Effect of gravity on capillary instability of liquid jets, Phys. Rev. E **87**, 053017 (2013).

[29] T. V. Vu, S. Homma, J. C. Wells, H. Takakura, and G. Tryggvason, Numerical simulation of formation and breakup of a three-fluid compound jet, J. Fluid Sci. Tech. **6**, 252 (2011).

[30] T. V. Vu, H. Takakura, J. C. Wells, and T. Minemoto, Pattern formation of hollow drops from final breakup of a hollow jet, J. Fluid Sci. Tech. **6**, 823 (2011).

[31] J. M. Gordillo and M. Perez-Saborid, Aerodynamic effects in the break-up of liquid jets: On the first wind-induced break-up regime, J. Fluid Mech. **541**, 1 (2005).

[32] M. A. Herrada, C. Ferrera, J. M. Monatenro, and A. M. Ganan-Calvo, Absolute instability in capillary jets, Phys. Fluids **22**, 064104 (2010).

[33] H. Gonzalez and F. J. Garcia, The measurement of growth rates in capillary jets, J. Fluid Mech. **619**, 179 (2009).

[34] M. A. Herrada, J. M. Monatenro, C. Ferrera, and A. M. Ganan-Calvo, Analysis of the dripping-jetting transition in compound capillary jets, J. Fluid Mech. **649**, 523 (2010).

[35] V. Theofilis, Global linear instability, Ann. Rev. Fluid Mech. **43**, 319 (2011).

[36] U. S. Sauter and H. W. Buggisch, Stability of initially slow viscous jets driven by gravity, J. Fluid Mech. **533**, 237 (2005).

[37] M. Rubio-Rubio, A. Sevilla, and J. M. Gordillo, On the thinnest steady threads obtained by gravitational stretching of capillary jets, J. Fluid Mech. **729**, 471 (2013).

[38] L. de Luca, M. Costa, and C. Caramello, Energy growth of initial perturbations of two-dimensional gravitational jets, Phys. Fluids **14**, 289 (2002).

[39] A. Javadi, J. Eggers, D. Bonn, M. Habibi, and N. M. Ribe, Delayed Breakup of Falling Viscous Jets, Phys. Rev. Lett. **110**, 144501 (2013).

[40] J. Uddin and S. P. Decent, Breakup of inviscid compound liquid jets falling under gravity, J. Phys. A **43**, 485501 (2010).

[41] M. Mohsin, J. Uddin, S. P. Decent, and M. F. Afzaal, Temporal instability analysis of inviscid compound jets falling under gravity, Phys. Fluids **25**, 012103 (2013).

[42] M. F. Afzaal, Breakup and instability analysis of compound liquid jets, Ph.D. thesis, University of Birmingham, 2014.

[43] N. P. Bali and N. Iyengar, *A Textbook of Engineering Mathematics* (Laxmi Publications, New Delhi, 2005).